

Synthesis of cobalt ferrite nanoparticles by co-precipitation at ambient and hydrothermal conditions

Arūnas Jagminas*,

Marija Kurtinaitienė,

Kęstutis Mažeika

*State Scientific Research Institute
Center for Physical
Sciences and Technology,
Savanorių 231,
LT-02300 Vilnius,
Lithuania*

We report the peculiarities of the synthesis of cobalt ferrite nanoparticles by complex-assisted co-precipitation route under ambient pressure in argon atmosphere and under increased pressure conditions. $\text{Co}_x\text{Fe}_{3-x}\text{O}_4$ nanoparticles with x from 0.3 to 1.0 in size of 1–20 nm were fabricated. The impact of the solution composition and reaction conditions on the size and stoichiometry of cobalt ferrite nanoparticles obtained were evaluated. Finally, the influence of post-growth treatments, such as washings, neutralization and centrifugations, on the hydrodynamic size of nanoparticles is presented and discussed. The nanoparticles were characterized by means of transmission and high resolution transmission electron microscopy (TEM, HRTEM), energy dispersive X-ray, Mössbauer and dynamic light scattering spectroscopy and atomic force microscopy (AFM).

Key words: co-precipitation, ferrites, nanoparticles, characterization

INTRODUCTION

The spinel ferrites with the formula $\text{Co}_x\text{Fe}_{(3-x)}\text{O}_4$ possess high saturation magnetization, coercivity, specific capacity and excellent thermal and chemical resistance. Due to these properties Co ferrite thin layers and nanostructured assemblies are studied for prospective applications in high-density magnetic devices [1, 2], Li^+ -batteries [3, 4], biosensing and nanomedicine [5–7]. In all of these applications the key point is uniformity of each nanoparticle composition and size. Besides, the required size and size dispersal of ferrite nanoparticles depend on the application field and tasks moved out. For example, magnetic resonance imaging needs nanoparticles in size less than 10 nm while cancer therapy hyperthermia applications need magnetic nanoparticles in size within the 20 to 50 nm range with a narrow size distribution [8, 9]. As reported, the synthesis path of ferrite nanoparticles is crucial in controlling their composition, shape, size and magnetic properties [10, 11] because other phases, in particular hydroxides, oxyhydroxides, or oxides, can be formed depending on the reaction conditions [12].

Several approaches have been reported to date for the synthesis of Co ferrite species in a variety of shapes and sizes. These include sol-gel [13–15], freeze drying [16], reverse micelle [17], co-precipitation [18, 19], template-assisted [20], solvothermal [21], hydrothermal [4, 22], Langmuir-Blodgett [23] and thermal destruction [24]. During the past decade, the significant progress has been also achieved in the synthesis of monodispersed Co ferrite nanoparticles [24–29]. However, the clear understanding of relationships between the size, composition and synthesis protocols of Co ferrite nanoparticles is not achieved until now. Therefore, it is difficult to synthesize predictable stable ferrofluids from desired cobalt ferrite nanoparticles as well as explain different behaviour of nanoparticles, fabricated by different paths, although comprised of the same composition and size. We suspect that it could be associated with the complexity of Co ferrites possessing a partially inverse spinel structure: $(\text{Co}_\delta\text{Fe}_{(1-\delta)})[\text{Co}_{(1-\delta)}\text{Fe}_{(1+\delta)}]\text{O}_4$, where δ depends on the synthesis history [30, 31]. Driven by these facts, we report here the synthesis of superparamagnetic Co ferrite $\text{Co}_x\text{Fe}_{(3-x)}\text{O}_4$ nanoparticles with x from 1.0 to 0.3, by convenient Massart's [32] and hydrothermal co-precipitation ways using Co(II) chloride and Fe(III) sulphate precursors, NaOH and various nanoparticle growth

* Corresponding author. E-mail: jagmin@ktl.mii.lt

stabilizers in an attempt to shed light on why these conditions influence the size, uniformity and composition of the products. We suspect that the results obtained in this study will help to synthesize cobalt ferrite nanoparticles possessing the required stoichiometry, size and stability during storage for months.

EXPERIMENTAL

All the reagents in this study were at least of analytical grade and, except NaOH, were used without any further purification. CoCl_2 , $\text{Fe}_2(\text{SO}_4)_3$, tartaric, citric, succinic, diglycolic, oleic and glutaminic acids were purchased from Aldrich Chemicals Inc. NaOH was purified by preparation of a saturate solution resulting in the crystallization of other sodium salts. Deionised distilled water was used throughout all experiments.

In this study, Co ferrite particles were synthesized in the thermostated glass reactor by co-precipitation method [32] from the complex-assisted alkaline solutions of Co(II) and Fe(III) salts at 70 to 85 °C and ambient pressure and from the same solutions autoclaved in a Teflon lined stainless steel autoclave, 25 mL in volume, at 110 to 130 °C, using 10 °C/min ramp, for up to 10 h. The working solutions were prepared from CoCl_2 and $\text{Fe}_2(\text{SO}_4)_3$ salts with the total concentration from 45 to 100 mmol/L at various mole ratios, NaOH and organic acids, such as citric, tartaric, diglycolic, D,L-glutaminic, oleic or succinic. The highest concentration of organic acids was fixed at 0.1 mol/L. All solutions were deoxygenated with argon before mixing. The pH of solutions was kept at from 10.0 to 13.0 by addition of 5.0 mol/L NaOH solution. The required quantity of NaOH solution in each case was determined by an additional blank experiment. In the subsequent experiment, this quantity was put into the reactor, composed with all other components, during several seconds under vigorous stirring. The synthesis in the thermostated reactor was conducted under a continuous argon gas bubbling. The crude products were centrifuged at 7 500 rpm for 5 min and carefully rinsed 5–6 times. The supernatants of last three centrifugations were connected and neutralized by addition of 0.1 mol/L citric acid down to $\text{pH} \cong 6.0$. The ferrofluid obtained was studied within the following week. The composition of synthesized products was investigated by energy dispersive X-ray spectroscopy (EDX) and following nanoparticles dissolution in HCl (1 : 1) solution by inductively plasma coupled optical emission spectrometry using OPTIMA 7000 DV (Perkin Elmer). Measurements were made on emission peaks at 238.89 nm and 259.94 nm for Co and Fe, respectively. Calibration curves were made from dissolved standards within 1 to 50 ppm concentrations in the same acid matrix as the unknowns. Standards and unknowns were analyzed at least 4 times. The detection limits based on three standard deviations resulted in $\pm 3.5\%$ error. X-ray powder diffraction experiments were performed on a D8 diffractometer (Bruker AXS, Germany), equipped with a Göbel mirror as a primary beam monochromator for CuK_α radiation.

Mössbauer spectra were collected in the transmission geometry from the spot of synthesized nanoparticles formed onto the shred of filter paper using $\text{Co}^{57}(\text{Rh})$ source. A closed cycle He cryostat (Advanced Research Systems, Inc.) was used for low temperature measurements. The hyperfine field B distributions and separate sextets or doublets were applied to fit the experimental spectra and determine the average hyperfine field $\langle B \rangle$ using WinNormos (Site, Dist) software. The transition temperature from the superparamagnetic to magnetic state is determined at temperature when $\langle B \rangle \approx 0.5B_0$, where B_0 is the maximum hyperfine field observed at the lowest temperature.

The morphology of as-grown products was investigated using a transmission electron microscope (TEM, model MORGAGNI 268) operated at an accelerating voltage of 72 keV. The nanoparticles subjected to TEM observations were dispersed in ethanol and drop-cast onto a carbon-coated copper grid. The average size of nanoparticles was estimated from at least 100 species observed in their TEM images. High resolution transmission electron microscopy (HRTEM) studies of as-synthesized products were performed using a LIBRA 200 FE at an accelerating voltage of 200 keV. The morphology of ultra small Co ferrite nanoparticles, spin coated onto the mica substrate, was investigated with an atomic force microscope Veeco AFM diInnova under a tapping mode. Hydrodynamic size of nanoparticles in water was determined by dynamic light scattering (DLS) tests at 25 °C under ambient conditions using Zeta sizer Nano S (Malvern Instruments, UK) equipment.

RESULTS AND DISCUSSION

Synthesis at ambient pressure

From the previous reports, the actual chemical composition of ferrites synthesized by co-precipitation depends on the composition of the solution applied, pH and the synthesis regime [33–37]. Therefore, in the first way, we sought to fabricate Co ferrite uniformly-sized nanoparticles by co-precipitation growth using CoCl_2 and $\text{Fe}_2(\text{SO}_4)_3$ salts solution containing additionally complexants and NaOH in an attempt to shed light why the composition of solution, pH and synthesis conditions influence the shape, size, size dispersity and composition of ferrite nanoparticles. Citric, tartaric, gluconic, diglycolic acid, etc. at concentrations up to 0.1 mol/L were employed as nanoparticle growth stabilizers in the synthesis reactions. The results obtained investigating the chemical composition of the products fabricated in this study from the degassed with argon alkaline solutions under variables of their compositions and conditions are presented in Table. As seen, different Fe-rich ferrites can be produced from these solutions, in which x varied between 0.3 and 1.0 depending on the composition of solution, pH and reaction temperature. AFM and TEM observations of the obtained ferrites indicated that the particles made in all investigated solutions are spherical and usually ultra small, e. g. between

Table. Variables of the composition of reaction products with the composition of solution and co-precipitation conditions at ambient pressure and Ar atmosphere

No.	Composition of solution, in mmol/L			Synthesis conditions			Resulted product
	CoCl ₂	Fe ₂ (SO ₄) ₃	Acid	pH	T, °C	Time, h	
1.	20	25	Citric, 90	11.5	70	5.0	Co _{0.71} Fe _{2.29} O ₄
2.	20	25	Diglycolic, 90	11.5	70	5.0	Co _{0.8} Fe _{2.2} O ₄
3.	20	25	Glutaminic, 50	11.5	70	5.0	Co _{0.9} Fe _{2.1} O ₄
4.	20	25	Succinic, 90	11.5	70	5.0	Co _{0.31} Fe _{2.69} O ₄
5.	20	30	Citric, 90	11.5	70	5.0	Co _{0.71} Fe _{2.29} O ₄
6.	20	40	Oleic, 90	11.5	70	5.0	Co _{0.92} Fe _{2.08} O ₄
7.	20	40	Diglycolic, 90	11.5	80	5.0	Co _{0.3} Fe _{2.7} O ₄
8.	54.5	45.5	Citric, 100	12.0	70	2.0	CoFe ₂ O ₄ + Co ₂ O ₃
9.	54.5	45.5	Citric, 100	12.0	85	2.0	CoFe ₂ O ₄
10.	50	50	Citric, 100	12.5	80	3.0	CoFe ₂ O ₄
11.	50	50	Citric, 100	12.0	85	2.0	CoFe ₂ O ₄
12.	47.5	52.5	Citric, 100	12.0	70	2.0	Co _{0.58} Fe _{2.42}
13.	50	50	Citric, 100	13.0	70	2.0	CoFe ₂ O ₄ + Co ₂ O ₃

1.0 and 2.5 nm (Fig. 1). The exception was obtained, however, using strongly alkaline solutions at pH ≥ 12.5 in which cobalt ferrite nanoparticles in an average size of ≥ 5 nm were fabricated. The typical XRD pattern of nanoparticles synthesized from alkaline solutions of CoCl₂ and Fe₂(SO₄)₃ in Ar atmosphere at elevated temperatures, ca 70–80 °C, is shown in Fig. 2A. The chemical analysis and EDX spectra collected from the scope of these nanoparticles showed Co and Fe to be present in approximately 1 : 2 ratio if the same concentrations (40–50 mmol/L) of Co(II) and Fe(III) precursors and pH 12–12.5 are used. The XRD pattern taken from the

same particles showed intensive and broad diffraction peaks centred at 2 θ 35.4°, 62.5°, 30.1° and 42.9° which according to International Centre Diffraction Data card number 04-005-7078 are attributable to (311), (440), (220) and (400) peaks of the CoFe₂O₄ polycrystalline spinel structure. We also found that in case of the molar ratio of CoCl₂/Fe₂(SO₄)₃ 1.2 : 1.0 in the initial mixture, along with the formation of CoFe₂O₄ some quantity of cobalt oxide was formed, as impurity. From these experiments, it was also concluded that among the applied additives citric and diglycolic acids are the most efficient for fabrication of cobalt ferrite nanoparticles with a narrow size

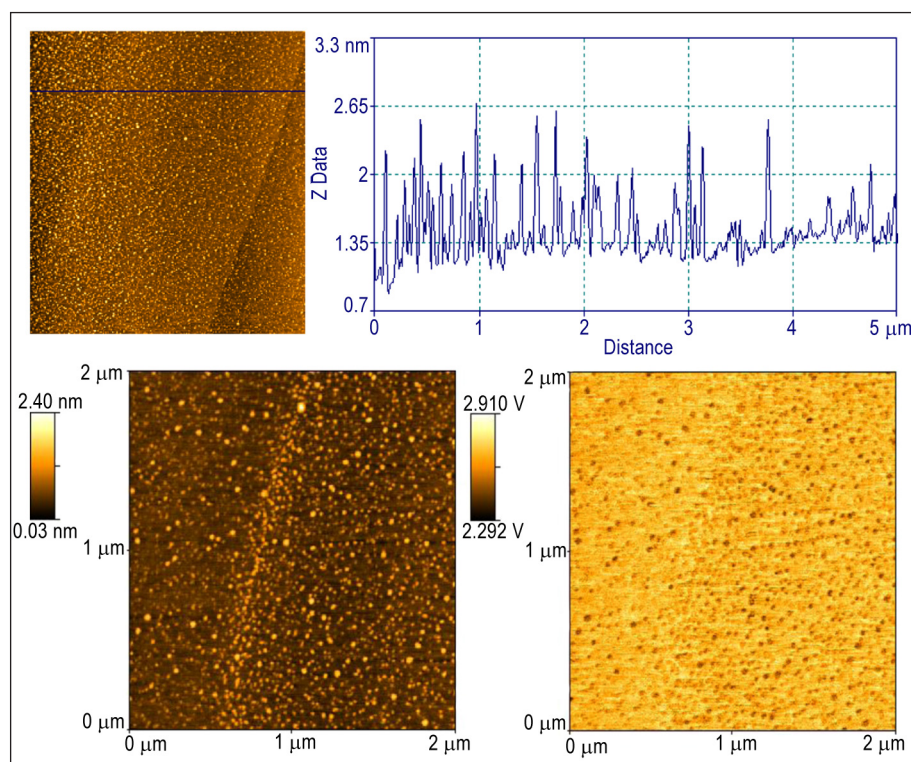


Fig. 1. AFM views and size profiles of Co ferrite nanoparticles (Nps) synthesized from the degassed with Ar solution containing 20.0 CoCl₂, 25.0 Fe₂(SO₄)₃ and 90 mmol/L citric acid and NaOH up to pH 11.5 at 70 °C for 5 h

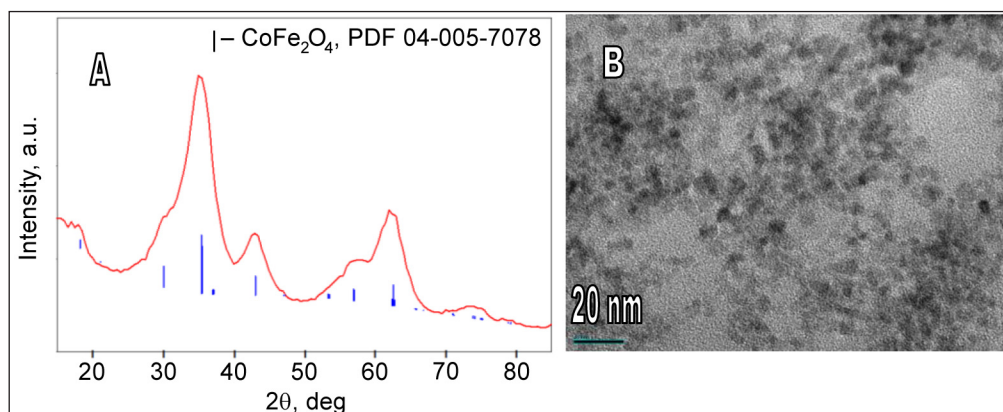


Fig. 2. A: XRD pattern of Co ferrite nanoparticles (B, TEM view) synthesized from the solution (in mmol/L): 50.0 CoCl_2 , 50.0 $\text{Fe}_2(\text{SO}_4)_3$, 100 citric acid and NaOH up to pH 12.5 in Ar atmosphere at 80 °C for 3 h. Mean size of N_{ps} ~ 5.0 nm

distribution. Furthermore, the aqueous ferrofluids produced from these cobalt ferrite nanoparticles are especially stable for months without any additional functionalization of their surface.

Synthesis under increased pressure

A significant size increase of ferrite nanoparticles was, however, observed when subjecting the synthesis under the hydrothermal conditions from the same solutions (Fig. 3). By this approach and the subsequent washing/centrifugation procedures, cobalt ferrite nanoparticles in an average size of from 7 to 20 nm were formed. HRTEM images (Fig. 3B) implied that cobalt ferrite nanoparticles obtained under

increased pressure conditions are polycrystalline. The stoichiometry of cobalt ferrite depends on the concentrations of Co(II) and Fe(III) salts and the pH of the solution applied. Increase in the pH results in the formation of more Co-rich nanoparticles. We note that in the past similar results were obtained fabricating magnetite nanoparticles from the alkaline Fe(II) and Fe(III) solution by hydrothermal treatment [38].

Mössbauer spectra

Room temperature Mössbauer spectra (MS) of cobalt ferrite nanoparticles synthesized by citric acid-assisted co-precipitation from degassed alkaline solutions of Co(II) and Fe(III)

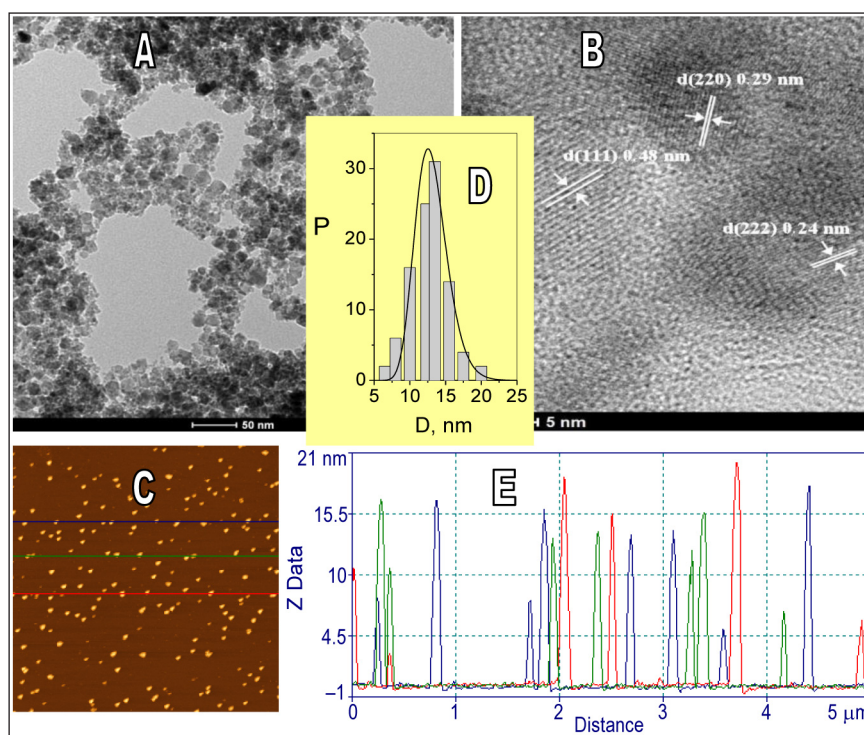


Fig. 3. TEM (A), HRTEM (B) and AFM (D) views of Co ferrite N_{ps} synthesized from the solution of 20.0 CoCl_2 , 25.0 $\text{Fe}_2(\text{SO}_4)_3$ and 90 mM citric acid and NaOH up to pH 11.5 at 130 °C for 10 h. E and D depict the size distribution histogram of these nanoparticles and AFM profiles, respectively

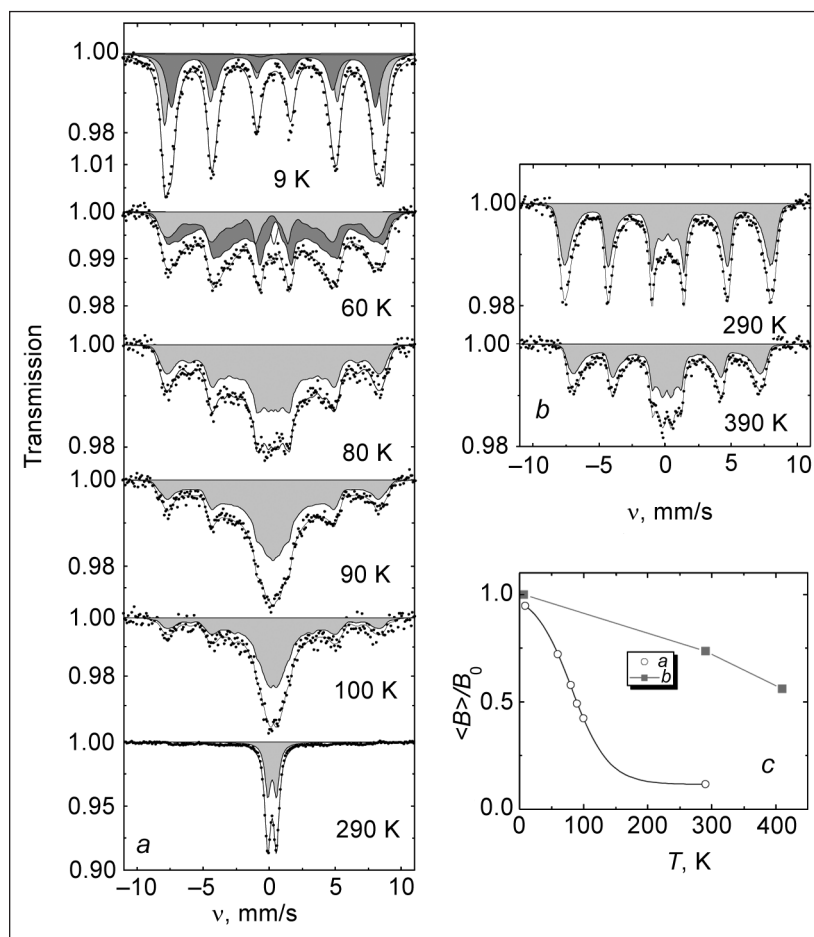


Fig. 4. Mössbauer spectra of cobalt ferrite *Nps* obtained by citric acid-assisted co-precipitation from alkaline (pH = 11.5) solution containing 50 CoCl₂, 50 Fe₂(SO₄)₃ and 100 mmol/L citric acid in argon atmosphere at ambient pressure and 70 °C for 5 h (a) and by autoclaving at 130 °C (b). In c the temperature dependences of relative hyperfine field of (a) and (b) *Nps* are shown

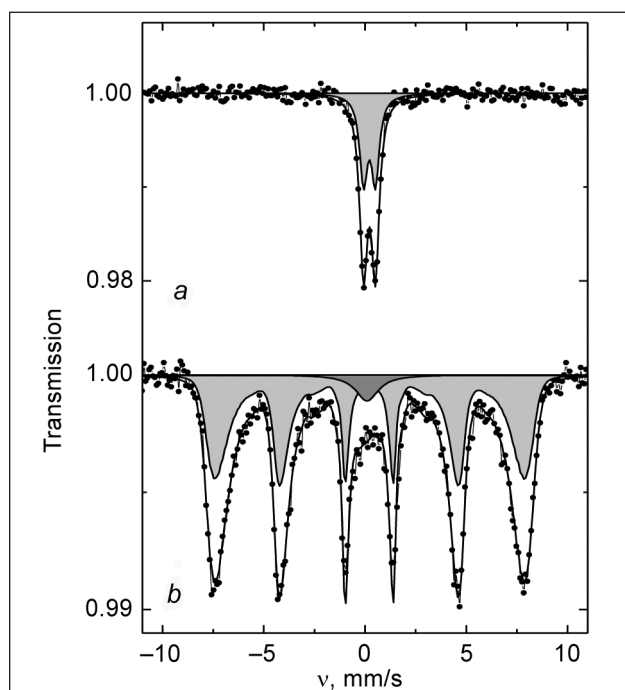


Fig. 5. Room temperature Mössbauer spectra of cobalt ferrite *Nps* synthesized in autoclave at 130 °C for 10 h by citric acid (100 mmol/L) assisted co-precipitation route from Co(II)/Fe(III) 1 : 1.25 solution at pH: a – 11.5, b – 12.75. The total concentration of metal salts 100 mmol/L. The composition of products: a – Co_{0.84}Fe_{2.16}O₄, b – Co_{0.94}Fe_{2.06}O₄

salts differ from those of nanoparticles synthesized from the same solution under increased pressure (Fig. 4). Variables in the composition of solution from 1.2 : 1.0 to 1 : 4 of Co(II)/Fe(III) precursors as well as the concentration of citric acid within 50 to 100 mmol/L range at pH up to 11.75 at the ambient pressure gave only ultra small nanoparticles independently on the synthesis time, varied from 2 to 10 h, and medium temperature within [70–85] °C range. Typical room temperature Mössbauer spectra of these nanoparticles are the symmetric doublets (Fig. 4a) characteristic of Co ferrites with average size <5 nm [39]. On the contrary, cobalt ferrite nanoparticles synthesized from the same solutions by hydrothermal approach are larger demonstrating sextets in their room temperature MS (Fig. 4b). It was determined, however, that both the composition and size of cobalt ferrite nanoparticles synthesized by hydrothermal treatment under the same conditions depend on the pH of reaction medium. Increase in the pH results in the formation of bigger and more Co-rich nanoparticles. These changes can also be seen from the room temperature Mössbauer spectra (Fig. 5) which demonstrate characteristic doublet or sextet-shaped MS for ultrafine (<5 nm) and larger nanoparticles, respectively [39].

A set of Mössbauer spectra of ultrafine cobalt ferrite nanoparticles at various temperatures down to cryogenic is depicted in Fig. 4a. From the analysis of these plots, the transition temperature of nanoparticles from the superparamag-

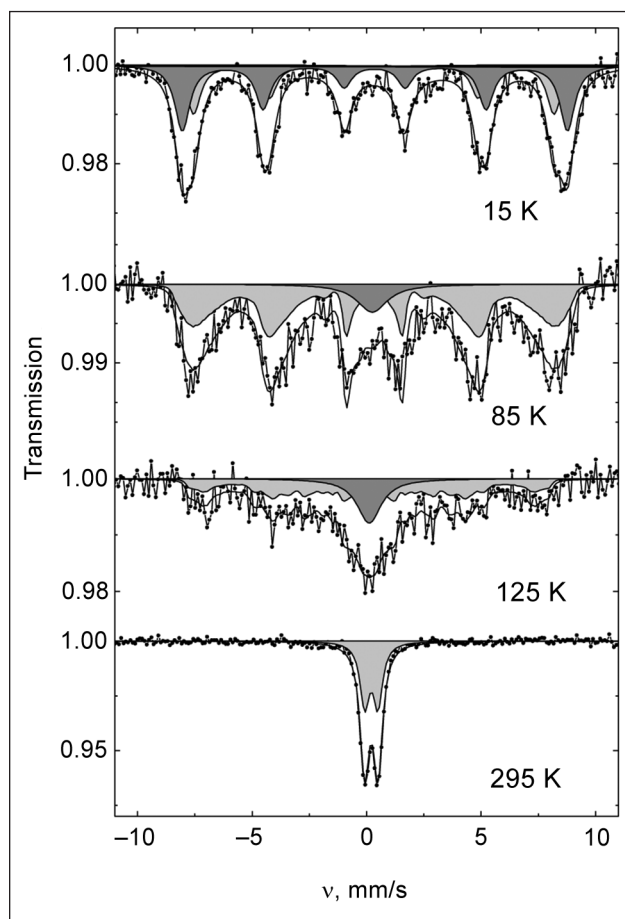


Fig. 6. Variables of the shape of Mössbauer spectrum of ultrafine Fe-rich cobalt ferrite Nps ($Co_{0.31}Fe_{2.69}O_4$) with measurement temperature. The synthesis was carried out in Co(II)/Fe(III) 1 : 2 alkaline (pH = 11.5) solution and ambient pressure at 80 °C for 5 h

netic to magnetic behaviour was determined; for $Co_xFe_{3-x}O_4$ ultrafine nanoparticles with $1.0 \geq x > 0.78$ this temperature is approximately 90 K which is much larger room temperature for nanoparticles obtained by autoclaving at 130 °C (Fig. 4).

It seems likely that the decrease in x results in the increase of transition temperature from the superparamagnetic to magnetic state (Fig. 6). Besides, through the increase of Fe(III) concentration in the reaction medium more Fe-rich nanoparticles can be produced. For example, in case of the molar ratio of Co(II)/Fe(III) 1 : 3, their total concentration of 100 mmol/L and pH = 11.5, extremely small cobalt ferrite nanoparticles with composition $Co_{0.3}Fe_{2.7}O_4$ were obtained in argon atmosphere at ambient pressure and 80 °C for 5 h. Mössbauer spectra taken from these nanoparticles revealed some higher transition temperature approximated to 115 K (Fig. 6).

Hydrodynamic size

Figure 7 depicts variables of the hydrodynamic size of cobalt ferrite nanoparticles dispersed in water on the post-growth processing steps. As seen, the size of as-grown at 70 °C for 3 h cobalt ferrite nanoparticles rinsed at least three times after centrifugation and separation from larger fractions varied within a quite wide range peaked at 258 nm. It seems likely that these nanoparticles are stabilized by attached OH^- ions because the pH of ferrofluid, stable for months, approximated 10.2. A quite large Z-average size (D_z) is somewhat surprising since from the AFM observations (Fig. 1) and Mössbauer spectra the true size of these nanoparticles is ≤ 5.0 nm. Neutralization of their medium to pH = 6.0 results in the surprising changes of D_z (curve 2). Besides, in this case two peaks of cobalt ferrite nanoparticles at 37.1 nm (40%) and

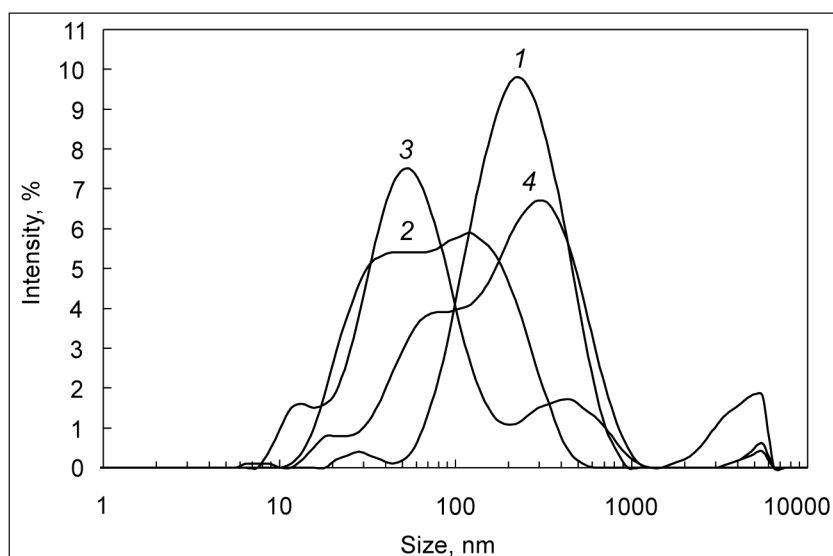


Fig. 7. Variables of the hydrodynamic size of cobalt ferrite Nps fabricated by citric acid-assisted co-precipitation route in argon atmosphere at 70 °C for 3 h on the post growth processing steps: 1 – as-grown and three times rinsed Nps in water, 2 – the same Nps following their neutralization with citric acid to pH = 6.0, 3 – the same Nps in supernatant after centrifugation and 4 – the same Nps rinsed again. The synthesis solution was composed of $CoCl_2$ (50 mmol/L), $Fe_2(SO_4)_3$ (50 mmol/L), 0.1 mol/L citric acid and NaOH up to pH = 12.0

146.3 nm (60%) ($D_z = 60.0$ nm) were distinguished. Again, through a subsequent centrifugation the larger fractions can be collected and quite uniform in size nanoparticles stabilized by citrate ions with $D_z = 55.0$ nm (curve 3) obtained. It is worth noting that further rinse (curve 4) results again in the formation of some part of aggregated nanoparticles with $D_z = 801$ nm. These observations suggest the conclusion for prospective storage of magnetic nanoparticles in neutralized ferrofluids.

CONCLUSIONS

This study utilizes a collection of principles in the predicting synthesis of cobalt ferrite nanoparticles by co-precipitation route under ambient and increased pressure conditions. Hence, we report here the design and composition variables of cobalt ferrite nanoparticles that can be obtained by citric acid-assisted co-precipitation way under ambient pressure and hydrothermal conditions from the alkaline solutions of Co(II) and Fe(III) salts kept at the pH from 10.0 to 13.0. We also note that at appropriate synthesis conditions both ultrafine (1–2.5 nm) as well as large, in size up to 20 nm, cobalt ferrite nanoparticles with general formula $\text{Co}_x\text{Fe}_{3-x}\text{O}_4$, where x varied within 0.3 to 1.0, can be obtained. Besides, variations of the hydrodynamic size of cobalt ferrite nanoparticles in water upon the rinsing, centrifugation and neutralization steps are presented and discussed. We also note that ultrafine cobalt ferrite nanoparticles are especially stable during storage in water for months and can be successfully applied for magnetic resonance imaging.

ACKNOWLEDGEMENTS

Support of this work by the Lithuania Science Council Foundation under Grant No. MIP-088/2011 is gratefully acknowledged. We also thank Rokas Kondrotas for his assistance in acquiring HRTEM images and Dr. Vidas Pakštis for XRD spectra collection.

Received 21 January 2013

Accepted 18 February 2013

References

1. Y. D. Meng, D. R. Chen, X. L. Jiao, *Eur. J. Inorg. Chem.*, **2008**, 4019 (2008).
2. Z. T. Chen, L. Gao, *Mater. Sci. Eng.*, **B 141**, 82 (2007).
3. Z. H. Li, T. P. Zhao, X. Y. Zhan, D. S. Gao, Q. Z. Xiao, G. T. Li, *Electrochim. Acta*, **108**, 2064 (2008).
4. Y. Wang, D. Su, A. Ung, J.-ho Ahn, G. Wang, *Nanotechnology*, **23**, 055402 (2012).
5. S. Loucrent, D. Forge, M. Port, A. Roch, C. Robic, L. Vander Elst, R. N. Muller, *Chem. Rev.*, **108**, 2064 (2008).
6. T. Kikumori, T. Kobayashi, M. Sawaki, T. Imai, *Breast Cancer Res. Treat.*, **113**, 435 (2009).
7. K.-C. Kim, E.-K. Kim, J.-W. Lee, S.-L. Maeng, Y. S. Kim, *Curr. Appl. Phys.*, **99**, 083908 (2006).
8. A. G. Roca, R. Costo, A. F. Rebolledo, et al., *J. Phys. D: Appl. Phys.*, **42**, 224002 (2009).
9. F. Gaseau, M. Levy, C. Wilhelm, *Nanomedicine*, **3**, 831 (2008).
10. M. Grigorova, H. J. Blythe, V. Blaskov, et al., *J. Magn. Magn. Mater.*, **183**, 163 (1998).
11. T. Ahn, J. H. Kim, H.-M. Yang, J. W. Lee, J.-D. Kim, *J. Phys. Chem. C*, **116**, 6069 (2012).
12. R. M. Cornell, U. Schwertmann, *Iron Oxides in the Laboratory*, VCH, Verlagsgesellschaft, Weinheim (1991).
13. N. Ch. Pramanik, T. Fujii, M. Nakanishi, J. Takada, *J. Mater. Chem.*, **14**, 3328 (2004).
14. P. Lavela, G. F. Ortiz, J. L. Tirado, E. Zhecheva, R. Stoyanova, S. Ivanova, *J. Phys. Chem. C*, **111**, 14238 (2007).
15. A. Gatelytė, D. Jasaitis, A. Beganskienė, A. Kareiva, *Materials Science (Medžiagotyra)*, **17**, 302 (2011).
16. P. Lavela, J. L. Tirado, M. Womes, J. C. Jumas, *J. Electrochem. Soc.*, **156**, A589 (2009).
17. C. Vidal-Abarca, P. Lavela, J. L. Tirado, *Solid State Ionics*, **181**, 612 (2010).
18. X. Yang, X. Wang, Z. Zhang, *J. Cryst. Growth*, **277**, 467 (2005).
19. S.-Y. Zhao, R. Qiao, X. L. Zhang, Y. S. Kang, *J. Phys. Chem. C*, **111(22)**, 7875 (2007).
20. Z. H. Li, T. P. Zhao, X. Y. Zhan, D. S. Gao, Q. Z. Xiao, G. T. Lei, *Electrochim. Acta*, **55**, 4594 (2010).
21. X. Jia, D. Chen, X. Jiao, T. He, H. Wang, W. Jiang, *J. Phys. Chem. C*, **112(4)**, 911 (2008).
22. N. Bao, L. Shen, W. An, P. Padhan, C. Turner, A. Gupta, *Chem. Mater.*, **21(14)**, 3458 (2009).
23. D. K. Lee, Y. H. Kim, Y. S. Kang, P. Stroeve, *J. Phys. Chem. B*, **109(31)**, 4939 (2005).
24. T. Hyeon, Y. Chung, J. Park, S. S. Lee, Y. W. Kim, B. H. Park, *J. Phys. Chem. B*, **106**, 6831 (2002).
25. C. R. Vestal, Z. J. Zhang, *Chem. Mater.*, **14**, 3817 (2002).
26. X. Jia, D. Chen, X. Jiao, T. He, H. Wang, W. Jiang, *J. Phys. Chem. C*, **112(4)**, 911 (2008).
27. E. Kang, J. Park, Y. Hg, M. Kang, J.-G. Park, T. Hyeon, *J. Phys. Chem. B*, **108**, 13932 (2004).
28. Q. Song, Z. J. Zhang, *J. Am. Chem. Soc.*, **126**, 6164 (2004).
29. N. Bao, L. Shen, W. An, P. Padhan, C. Turner, A. Gupta, *Chem. Mater.*, **21(14)**, 3458 (2009).
30. M. Grigorova, H. J. Blythe, V. Blaskov, et al., *J. Magn. Magn. Mater.*, **183**, 163 (1998).
31. M. Rajendran, R. C. Pulla, A. K. Bhattacharya, D. Das, S. N. Chintalapudi, C. K. Majumdar, *J. Magn. Magn. Mater.*, **232**, 71 (2001).
32. R. Massart, *IEEEA Trans. Magn.*, **16**, 178 (1980).
33. D. H. Lee, H. S. Kim, J. Y. Lee, C. H. Yo, K. H. Kim, *Solid State Commun.*, **96**, 445 (1995).
34. A. Franko Jr., V. Zapf, *J. Magn. Magn. Mater.*, **320**, 709 (2008).
35. A. Franko Jr., V. Zapf, *J. Appl. Phys.*, **101**, M506 (2007).
36. J. Park, N. J. Kang, Y. W. Jun, S. J. Oh, H. C. Ri, *J. Chem. Phys. Chem.*, **3**, 543 (2002).

37. S. Ayyappan, S. Mahadevan, P. Chandramohan, M. P. Srinivasan, J. Philip, B. Raj, *J. Phys. Chem. C*, **114**, 6334 (2010).
38. O. Horney, S. Neveu, S. de Montredon, J.-M. Siaugue, V. Cabuil, *J. Nanopart. Res.*, **11**, 1247 (2009).
39. S. W. Lee, C. S. Kim, *J. Magn. Magn. Mater.*, **303**, e315 (2006).

Arūnas Jagminas, Marija Kurtinaitienė, Kęstutis Mažeika

**KOBALTO FERITO NANODALELIŲ SINTEZĖ
KO-NUSODINIMO METODU APLINKOS IR
PADIDINTO SLĖGIO SĄLYGOMIS**

Santrauka

Tirti kobalto ferito superparamagnetinių nanodalelių (*Nd*) sudarymo ypatumai aplinkos ir padidinto slėgio sąlygomis. Sintezė atlikta šarminiuose CoCl_2 ir $\text{Fe}_2(\text{SO}_4)_3$ vandens tirpaluose, turinčiuose magnetinių *Nd* augimo procesą veikiančių rūgščių ar jų druskų. Keičiant tirpalų sudėtį ir sintezės sąlygas pagamintos tiek ultrasmulkios (1–3 nm), tiek smulkios (5–20 nm) $\text{Co}_x\text{Fe}_{3-x}\text{O}_4$ *Nd*, kuriose *x* gali kisti nuo 0,3 iki 1,0. Parodyta, kad aplinkos slėgio ir inertinių dujų aplinkos sąlygomis gali būti formuojamos itin smulkios 1–5 nm dydžio CoFe_2O_4 *Nd*. Tokie feroskysčiai yra itin stabilūs ir gali būti perspektyviai taikomi nanomedicinoje.